Research Square

Preprints are preliminary reports that have not undergone peer review.
They should not be considered conclusive, used to inform clinical practice,
or referenced by the media as validated information.

Morphological, behavioral and molecular studies on CRISPR/Cas9-mediated knockout of the *NOMO1* gene in zebrafish

Fei Li
Children's Hospital of Fudan University
Tingting Li
Children's Hospital of Fudan University
Jia Lin
Children's Hospital of Fudan University
Jing Jian
Children's Hospital of Fudan University
Qi Zhang
Children's Hospital of Fudan University
Yinglan Zhang
Children's Hospital of Fudan University
Xiuyun Liu
Children's Hospital of Fudan University
Yongxia Ji
Children's Hospital of Fudan University
Xu Wang
Fudan University Shanghai Cancer Center
Qiang Li (liq@fudan.edu.cn)
Children's Hospital of Fudan University https://orcid.org/0000-0002-8388-0968

Research

Keywords: Nomo1, CRISPR/Cas9, Zebrafish, Autism, Social behavior, Neurotransmitter, Functional mechanism

Posted Date: January 7th, 2021

DOI: https://doi.org/10.21203/rs.3.rs-54088/v2

License: This work is licensed under a Creative Commons Attribution 4.0 International License.
Read Full License

Abstract

Background: Multiple clinical genome-wide analysis identified that chromosome 16p13.11 is a hotspot associated with neuropsychiatric disorders such as autism, schizophrenia and epilepsy. *Nodal modulator 1 (NOMO1)*, located on human chromosome 16p13.11, was considered as a candidate gene with neuropsychiatric disorders. However, it is unknown whether the *nomo1* deficiency causes neurological abnormalities, and the molecular mechanisms and pathogenesis of the *NOMO1* gene remain unclear. To study the effects of *nomo1* deficiency on brain development and neuropsychiatric system, a *nomo1* knockout zebrafish model was established.

Methods: We developed a viable vertebrate model of *nomo1* loss-of-function using CRISPR/Cas9 technology and characterized *nomo1* mutant zebrafish. Phenotypic and functional studies of developing *nomo1* mutant zebrafish, including morphological measurements, behavioral assays, and functional mechanistic analyses, were performed.

Results: Morphological differences in the phenotype of *nomo1*$^{-/-}$ zebrafish gradually became less noticeable during development, however, the enlarged interstitial spaces in midbrain and hindbrain were detected in *nomo1* mutant zebrafish. Meanwhile, the *nomo1* deficiency caused the change of expression levels in neurotransmitters of γ-aminobutyrate, glutamate and serotonin. Interestingly, the *nomo1* loss-of-function zebrafish model exhibited social defects and repetitive behaviors in juvenile, which represented autism-like behaviors. The transcriptome analysis showed different gene expression patterns in mutant zebrafish at the genetic level. Further results revealed that the neuroactive drug PTZ recovered the decreased locomotor phenotype in larval mutant zebrafish.

Conclusions: In this study, we established a *nomo1* vertebrate animal model using CRISPR/Cas9 gene editing approach. The loss-of-function of *nomo1* displayed autism-like behaviors and altered levels of the γ-aminobutyrate, glutamate and serotonin in zebrafish, which provide evidence that *nomo1* as a candidate gene for autism. The versatility of zebrafish model is contributed to studying *NOMO1*-related disorders and conducting drug screening in future.

Limitations: Further studies are needed to determine whether an intervention with a neuroactive drug in *nomo1*$^{-/-}$ zebrafish to alter the behavioral phenotype is applicable to the behavior of human patients.

Background

Clinical genetic evidence supports the viewpoint that chromosome 16p13.11 is a hotspot associated with various neuropsychiatric disorders, such as epilepsy, autism spectrum disorder (ASD), schizophrenia, and attention deficit hyperactivity disorder (ADHD) [1-4]. *Nodal modulator 1* (*NOMO1*), a negative regulator of the nodal signaling pathway, is located on chromosome 16p13.11. In 2015, Tassano *et al.* described a 13-year-old Italian male patient with epilepsy, mental retardation, developmental disorders, and dysmorphic features who had paternally inherited interstitial deleted copy number variations (CNVs) in 16p13.11 using a comparative genomic hybridization (CGH) analysis [5]. In 2016, Brownstein *et al.* reported

evidence of a patient with psychosis who carried duplicated CNVs in 16p13.11 [6]. From the aboved research, we discovered that the *NOMO1* gene was included in relevant CNVs. Clinical studies suggest a potential role for *NOMO1* in neuropsychiatric disorders; however, the contributing factors explaining how *NOMO1* deficiency results in neuropsychiatric disorders remain unclear.

Nodals are essential for formation of the neuroectoderm and mesoderm during the development of early embryos. NOMO1, TMEM147 and nicalin form protein complexes that inhibit the nodal signaling pathway during the early development of zebrafish [7-9]. *NOMO1* is a candidate gene associated with glioma, early-onset colorectal cancer and facial asymmetry [10-12]. In 2018, Cao *et al.* constructed a *nomo1* knockout (KO) zebrafish model that exhibited hypoplasia and dysmorphism symptoms with a phenotype similar to chondrodysplasia in humans [13]. By determining the expression pattern of *nomo1* in zebrafish using *whole-mount in situ hybridization* (WISH), the *nomo1* gene was shown to be expressed at high levels in the anterior mesendoderm and endoderm during early embryonic development and was abundant in the brain of larval zebrafish [9, 13]. However, none of these studies present evidence to directly link *nomo1* deficiency with the nervous system in an animal model.

Abnormalities in the nervous system can lead to different neuropsychiatric disorders. Neuropsychiatric disorders are complex developmental diseases that seriously affect the health of affected individuals and reduce the life quality of patients. Patients with neuropsychiatric disorders usually present various behavioral phenotypes. For example, ADHD patients exhibit characterization of inattention, hyperactivity and increased impulsivity [14]. ASD is characterized by various subtypes of social deficits and the presence of repetitive stereotypic behaviors and restricted interests [15]. In the field of neuropsychiatry, ASD is one of the widely concerned diseases, which have estimated to impact more than 1% of the population [16]. The genetic factors play an important role in the pathogenesis of ASD [17]. The diagnoses of ASD are mainly depends on the clinical characteristics, however, comorbidities are common throughout patients' lives [18, 19]. The biological basis of ASD is not fully understood. Therefore, animal model is a powerful tool to study the pathogenesis of ASD.

Zebrafish have been accepted and applied to functional mechanistic studies of neuropsychiatric disorders as vertebrate model organisms. Researchers have established detection and analytical methods to measure the characteristic behavioral phenotypes, including locomotion, thigmotaxis, social behavior and aggressive behavior, in zebrafish [20, 21]. The CRISPR/Cas9 technique is widely used for gene editing, and a number of transgenic zebrafish models have been developed [13, 22-24]. Notably, zebrafish models exhibit ASD-like phenotypes similar to those observed in human diseases. For example, *dyrk1aa* KO zebrafish exhibit social behavior impairments that reproduce human phenotypes of ASD in a vertebrate animal model [25]. Knockout of the *shank3b* gene via CRISPR/Cas9 resulted in autism-like behaviors and an enlarged ventricles size in zebrafish, which is retrospect the Phelan-McDermid syndrome (PMS) patients that frequently reported in human [22].

We established an in vivo KO model using zebrafish to understand the functional mechanisms underlying *nomo1* deficiency and neuropsychiatric disorders. In the present study, *nomo1* deficiency in zebrafish

causes abnormal development of central nervous system. Meanwhile, the *nomo1* mutant zebrafish exhibit social defects and repetitive behaviors at 2 months postfertilization (mpf), which represented autism-like behaviors. Additionally, we reported how *nomo1* deficiency conspicuously influences brain development and neurotransmitter metabolism in zebrafish. These results represent a comprehensive study of the mechanistic link between *nomo1* deficiency and ASD-like phenotypes and highlight the critical role of *nomo1* in brain development of zebrafish.

Methods

Zebrafish breeding and the generation of *nomo1* mutant zebrafish

Wild-type (WT) zebrafish of the Tuebingen (TU) strain were provided by the zebrafish facility of the Translational Medical Center for Development and Disease, Shanghai Key Laboratory of Birth Defect, Institute of Pediatrics, Children's Hospital of Fudan University. The zebrafish were raised in a circulating water system with a water temperature of 28.5°C and 14 h of light and 10 h of darkness per day (8:00-22:00, light). Zebrafish breeding, feeding and spawning were conducted strictly in accordance with the Zebrafish Book (http://zfin.org/zf_info/zfbook/zfbk.html).

The detailed CRISPR/Cas9-mediated editing method was performed using standard procedures [26, 27]. A synthetic specific guide RNA (sgRNA) and Cas9 mRNA (concentrations of 30 ng/μL and 300 ng/μL, respectively) in a total volume of 3 nL were coinjected into every WT zebrafish embryo at the single-cell stage. Genomic DNA was extracted, and genotyping samples were screened for the mutation frequency by comparison with WT zebrafish samples. The primer sequences used for genotyping are shown in Table S1. The mutant chimeric zebrafish were mated with the TU strain to purify the background and obtain *nomo1*$^{+/-}$ zebrafish. Male and female *nomo1*$^{+/-}$ zebrafish were crossed to acquire *nomo1*$^{+/+}$, *nomo1*$^{+/-}$, and *nomo*$^{-/-}$ littermates. We collected multiple batches of littermates produced by *nomo1*$^{+/-}$ zebrafish for the phenotypic analysis to obtain a sufficient number of embryos.

RT-qPCR

Total RNAs were extracted from embryos, heads and the brain tissues of zebrafish at different developmental stages using TRIzol reagent (Ambion, USA). Genomic DNA was removed by DNase I, and total RNA (1 μg) was reverse transcribed using a PrimeScript cDNA Synthesis Kit (TaKaRa, Japan). RT-qPCR was conducted with a LightCycler® 480 apparatus (Roche, Germany) and SuperReal PreMix Plus (Tiangen, China) according to the manufacturers' instructions. The fold changes in RNA levels were calculated using the ΔΔCt method. The RT-qPCR primer sequences are listed in Table S1.

WISH

The targeted DNA was cloned into the pGEM-T Easy vector, and probes were synthesized using a linearized plasmid through in vitro transcription with the DIG-RNA labeling Kit (Roche, Austria). The related primers of synthetic probes are shown in Table S1. Embryos of WT and mutant zebrafish were

collected at different stages (12 hpf, 24 hpf and 48 hpf) and fixed with 4% paraformaldehyde at 4°C overnight. WISH was performed as previously described [23], and images were captured and processed using a Leica 6000 microscope.

Drugs

Pentylenetetrazole (PTZ) (Sigma-Aldrich; P6500, St. Louis, MO) was dissolved in ultrapure water to prepare a 32 mM stock solution that was frozen at -80°C. The PTZ working solution was diluted to the appropriate concentration with system water prior to the experiments.

Behavioral assays in mutant zebrafish

Locomotion and thigmotaxis tests

Behavioral assays of larval zebrafish were performed at 28.5°C in 24-well plates (Fig. 2G), and the inner diameter of each well was 18 mm, providing the larvae sufficient space to swim. The 24-well plates were then placed in a Zebrabox (ViewPoint Life Sciences, Lissieu, Calvados, Lower Normandy Region, France) that recorded videos tracking the larval zebrafish. The experimental procedure consisted of 55 min of continuous illumination with light at an intensity of 100 lx and two 10-min light-dark transition cycles for a total time of 75 min to elicit a photomotor response (PMR) (Fig. 2A). The experiment examined both spontaneous movement and changes due to lighting transitions. The data were quantified with ZebraLab software (ViewPoint Behavior Technology, France), the video rate was set to 25 frames per second (fps), and the frames were pooled into 1-min time bins. The threshold was set to 29, a suitable level to accurately detect the trajectory of larval zebrafish in motion.

Zebrafish at 15 days postfertilization (dpf), 30 dpf and 2 mpf swam freely in the open field at 28.5°C, and the experimental time was 30 min. Behavioral recording began after an adaptation period (1-2 min) when the zebrafish acclimated to the environment. Zebrafish at 15 dpf were examined in a 9-cm diameter dish since they were a smaller size (Fig. 3A). Zebrafish at 30 dpf and 2 mpf were examined in a novel tank (inner dimensions, 30 × 30 × 20 cm) (Fig. 3C). The collected data were exported using ZebraLab software.

Social and repetitive behavior tests

The individual social behavior (social preference behavior) and group social behavior (shoaling behavior) of juvenile zebrafish (2 mpf) were assessed at 28.5°C. A single zebrafish was placed on one side of a standard mating tank (inner dimensions, 21 × 10 × 7.5 cm), and another six WT zebrafish were placed on the other side of the mating tank and separated from the single zebrafish by a transparent plastic plate to examine social preference behavior (Fig. 4A). Region 1 was regarded as a social area, whereas Region 2 was regarded as a nonsocial area, and the experiment lasted for 30 min. Behavioral recording began after an adaptation period (1-2 min) when the zebrafish acclimated to the tank. The behavior of the zebrafish was quantified as a distribution of distances or regions adjacent to the group. The ratio of the time the zebrafish stayed in the social area and the distance spent away from the social area directly reflects the social activity of a single juvenile zebrafish.

For the shoaling test, six WT zebrafish (or six *nomo1*$^{-/-}$ zebrafish) were acclimated to a novel tank (inner dimensions, 30 × 30 × 20 cm) (Fig. 4F). A camera recorded the trajectory of the experimental zebrafish over 30 min, and the adaptation period was 1-2 min. The indicator of inter-individual distance was used to assess the average distance between each zebrafish in the shoal [22, 28].

We observed different types of repetitive behavior (back-and-forth motions, stereotypic movement and large circular movement) in the *nomo1*$^{-/-}$ zebrafish (Fig. 4H) when we examined the spontaneous movement of juvenile zebrafish. All the repetitive behavior tests began after an adaptation period (1-2 min) when the zebrafish acclimated to the tank. Back-and-forth motion was defined as moving one time on one edge or adjacent edges of the tank and returning to the origin. Stereotypic movement referred to repeated movement of the zebrafish in a small area, where the maximum movement distance from the beginning to the end was less than 30 mm and continuous swimming time was greater than 5 s. Large circular movement referred to the swimming of the zebrafish in a counterclockwise or clockwise circle along the edges of the tank. After the stereotypic movements were defined, the data were obtained objectively by a computer program within the experimental period.

Kin recognition test

The mating tank, the specifications of which were the same as the tank used in the social preference test, was divided into three compartments using transit plates to examine kin preference behavior. Three zebrafish of the same strain and same age were placed on one side of the tank, and three red zebrafish of different strains were placed on the other side of the tank. The juvenile WT and mutant zebrafish were placed in the middle area of the tank (Fig. S3A). Region A was regarded as the kin preference area, whereas Region B was regarded as the non-kin preference area. Behavioral recording began after an adaptation period (10 min) when the zebrafish adapted to the tank. Videos were recorded for 30 min. The time spent/distance moved ratio for the zebrafish that stayed in the Region A was used to measure the ability of kin recognition in zebrafish.

Preparation of paraffinized sections and HE staining

The brain tissues of adult zebrafish (3 mpf) were completely removed under a microscope and immersed in 4% paraformaldehyde for 24 h. Tissues were dehydrated and transparentized with the following conditions and protocol: 70% ethanol, 30°C, 30 min; 95% ethanol, 30°C, 10 min; 95% ethanol, 30°C, 10 min; 100% ethanol (I), 30°C, 10 min; 100% ethanol (II), 30°C, 10 min; xylene (I), 30°C, 30 min; and xylene (II), 30°C, 30 min. The tissues were waxed and embedded using a paraffin embedding station (Leica EG1150H) for 3 h at 65°C. Then, a microtome (Leica RM2235) was used to produce continuous slices at a thickness of 4 μm. The slices were floated in 40°C warm water to flatten their surfaces, and then baked in a 60°C oven. HE staining was performed by staining with hematoxylin and eosin for 5 min each. Photographs were taken with a Leica 205C microscope.

Targeted metabolomics analysis of neurotransmitter

Juvenile zebrafish were frozen in liquid nitrogen and placed on ice. Under the microscope, the brains were directly removed with a surgical blade, and 10 brains were placed in an Eppendorf (EP) tube. Selective/multiple reaction monitoring assays (SRM/MRM), which is based on liquid chromatography-tandem mass spectrometry (LC-MS/MS), has been used to simultaneously detect neurotransmitters in animals. LC-MS/MS can determine absolute quantitative amounts of target metabolites with strong specificity and high sensitivity and accuracy [29, 30].

Brain tissue samples were added to 1 mL of methanol/acetonitrile/ultrapure water (2:2:2, v/v/v), vortexed and ultrasonicated. After an incubation at -20°C for 30 min, the precipitated proteins were centrifuged at 14,000 rcf for 4 min at 4°C. The supernatant was removed and dried in vacuo. For spectrometric detection, 100 µL of an acetonitrile/water solution (1:1, v/v) were used to reconstitute the pellet, which was centrifuged at 14,000 rcf for 4 min at 4°C, after which the supernatant was collected for analysis. Samples were separated using an Agilent 1290 Infinity LC Ultra Performance LC System. Mass spectrometry was conducted in negative ion mode using a 5500 QTRAP mass spectrometer (AB SCIEX) for analysis. Data on stability and repeatability were evaluated using cluster and statistical analyses.

HPLC

High-performance liquid chromatography (HPLC) was also employed to examine the levels of norepinephrine, dopamine (DA), 3,4-dihydroxyphenylacetic acid (DOPAC), and serotonin (5-HT) in the brains of juvenile zebrafish. The samples were suspended in ice-cold PBS (20 µL/sample) and ground completely. Then, the samples were centrifuged at 11,900 rpm at 4°C for 10 min, and the protein content of 1 µL of the supernatant from each sample was quantified. The remaining supernatants were added to 2 µL of perchloric acid (0.2 N) and centrifuged again at 11,900 rpm at 4°C for 10 min. The supernatant was collected and stored at -80°C. The HPLC analysis was performed using an Agilent 1200 HPLC system (Agilent, USA) with Antec DECADE SDC electrochemical detector (Antec, the Netherlands). The expression levels of neurotransmitters were normalized to the protein content.

Transcriptomics

The total RNA was extracted from each sample of brain tissue from juvenile zebrafish using TRIzol reagent (Ambion, USA) according to the manufacturer's instructions. RNA degradation and contamination were monitored on 1% agarose gels. The RNA concentration was measured using a Qubit® RNA Assay Kit with a Qubit®2.0 fluorometer (Life Technologies, CA, USA), and RNA integrity was assessed using an RNA Nano 6000 Assay Kit of the Bioanalyzer 2100 system (Agilent Technologies, CA, USA). Three micrograms of RNA per sample was used as the input for RNA sample preparation. Sequencing libraries were generated using a NEBNext® Ultra™ RNA Library Prep Kit for Illumina® (New England Biolabs, USA) according to the manufacturer's recommendations, and index codes were added to attribute sequences to each sample. PCR products were then purified (AMPure XP system), and library quality was assessed using the Agilent Bioanalyzer 2100 system. Sequencing fragment data detected using a high-throughput sequencer was converted from image data into sequence data (reads) containing sequence information

from each sequenced fragment and its corresponding sequencing quality by CASAVA base recognition. High-quality reads were aligned to the zebrafish reference genome (GRCz11) using HISAT2 v2.0.5. Differentially expressed genes (DEGs) were identified using the DESeq2 R package (1.16.1), which uses statistical methods to determine differential expression from digital gene expression data using a model based on a negative binomial distribution. The resulting p-values were adjusted using the Benjamini and Hochberg approach for controlling the false discovery rate. Genes with an adjusted p-value <0.05 according to DESeq2 were defined as DEGs. In addition, a Gene Ontology (GO) enrichment analysis of the DEGs was implemented by the clusterProfiler R package, which corrected the gene length bias. GO terms with corrected p-values <0.05 were considered significantly enriched in DEGs. The Kyoto Encyclopedia of Genes and Genomes (KEGG) database is a resource used to understand high-level functions and utilities of biological systems, such as a cell, an organism and an ecosystem, and it is specifically focused on analyzing large-scale molecular datasets generated by genome sequencing and other high-throughput experimental technologies (http://www.genome.jp/kegg/). We used the clusterProfiler R package to assess the statistically significant enrichment of DEGs in KEGG pathways.

Statistical analysis

The experimental data in this study were analyzed and mapped with GraphPad Prism 6.0 software. Values are presented as the means ± SEM. Differences between two groups were analyzed using paired Student's t-test and corrected Student's t-test, and p-values <0.05 indicated a significant difference.

Results

The *nomo1* mRNA expression level from early embryonic development to the juvenile stage and generation of *nomo1* mutant zebrafish

The *nomo1* gene in zebrafish is homologous to the human *NOMO1* gene, and they share 68% and 70% identity in cDNA and protein sequences, respectively. Cao *et al.* and Haffner *et al.* have confirmed the expression pattern of *nomo1* from early embryonic development to larval stages in zebrafish using WISH [9, 13]. RT-qPCR was performed to determine the expression level of *nomo1* during different developmental stages. At 12 hpf-7 dpf, whole zebrafish embryo were used since they were a smaller size. At 14 dpf, heads of zebrafish were used and at 1-2 mpf, the brain tissues were studied. The expression of the *nomo1* mRNA in embryonic zebrafish increased before 48 hpf and decreased at 5 dpf and 7 dpf, as determined using RT-qPCR (12 hpf-7 dpf). As development progressed, the expression of the *nomo1* mRNA peaked a second time at 14 dpf, and the highest mRNA expression level was detected in brain tissues from 2 mpf zebrafish (Fig. 1F).

The sgRNA of *nomo1* was designed by editing exon 7, which was located before the functional structural domain FN3 in the genomic sequence of zebrafish [31]. The sequence was 5'- GGG CTA TGA TGT CTC TGG AG- 3' (Fig. 1A). Fig. 1B-D shows the process by which *nomo1* homozygous zebrafish were generated using CRISPR/Cas9 technology. Genomic DNA was extracted, and the specific PCR products were sequenced, confirming that the *nomo1* sequence contained a 1-base deletion (Fig. 1E), resulting in a

frameshift mutation and truncated protein 10 amino acids after the mutation (Fig. 1H). The abnormal *nomo1* mRNA expression level was detected in mutant zebrafish at 48 hpf, 14 dpf and 2 mpf, as determined using RT-qPCR (Fig. 1G).

Morphological analysis of *nomo1*$^{-/-}$ zebrafish

We measured morphological changes in mutant zebrafish to examine the consequences of *nomo1* deficiency during zebrafish development (Fig. S1). The mortality of the early mutant embryos (24 hpf) was higher than WT zebrafish (Fig. S1H). Mutant embryos exhibited the following morphological changes during development: developmental retardation (the extended rupture of membranes), tail bending (Fig. S1D, arrow), pericardial edema (Fig. S1E, arrow) and developmental malformation (Fig. S1F). The ratios of morphological changes are shown in Fig. S1H. However, these morphological differences in the phenotype of *nomo1*$^{-/-}$ zebrafish gradually became less noticeable during development (Fig. S1A-C). We statistically analyzed the body length of zebrafish at different developmental stages and did not observe a significant difference (Fig. S1G).

Nomo1 deficiency significantly affected the locomotion of 7 dpf zebrafish under different illumination intensities

We examined the locomotor activity of 7 dpf zebrafish and their reactions to light-dark transitions to determine whether the loss-of-function of *nomo1* would modulate the behavior of larval zebrafish. After 20 min of adaptation, the locomotion and thigmotaxis behaviors of larval zebrafish were analyzed (Fig. 2A). We recorded the trends in the swimming behaviors of WT and mutant zebrafish in 24-well plates (Fig. 2B). An analysis of the average distance moved per minute from minutes 21 to 60 (L0) under light conditions (Fig. 2C) showed that the locomotion of *nomo1*$^{-/-}$ zebrafish was significantly reduced compared with *nomo1*$^{+/+}$ zebrafish, confirming the specificity of the phenotype.

Similarly, the mutant zebrafish displayed significantly decreased locomotor activity during the two light-dark cycles, and WT and mutant zebrafish showed a light-sensitive reaction in every light-dark cycle (Fig. 2D-E). Although the WT and mutant zebrafish showed photosensitivity in the two light-dark cycles, the mutant zebrafish had a more intense response to lighting changes in the first light-dark cycle than WT zebrafish, whereas no statistically significant differences in photosensitivity were observed in the second light-dark cycle (Fig. 2F).

In addition, we measured the thigmotaxis of WT and mutant zebrafish under light conditions by recording the percentage of time spent/distance moved in the inner zone (Fig. 2G). The *nomo1* mutant zebrafish exhibited an edge preference under continuous illumination, indicating increased thigmotaxis behavior (Fig. 2H).

The 15 dpf and 30 dpf *nomo1*$^{-/-}$ zebrafish showed increased locomotion

We also analyzed the locomotion of *nomo1*$^{-/-}$ zebrafish during development. A different sized container was used for 15 dpf and 30 dpf zebrafish, and the trajectories of the zebrafish are shown in Fig. 3A and 3C. The diagram shows a trend in the swimming behavior of WT and mutant developing zebrafish during the experimental period (Fig. 3B, D, and E). The locomotor activity of 15 dpf and 30 dpf zebrafish was significantly enhanced. The average distance moved per minute was not significantly different between *nomo1*$^{-/-}$ zebrafish and WT zebrafish at 2 mpf (Fig. 3F).

Juvenile *nomo1*$^{-/-}$ zebrafish exhibited autism-like behaviors

The social preference behavior (Videos S1-S2) and shoaling behavior (Videos S3-S4) were visually presented in the form of videos. The *nomo1*$^{+/+}$ zebrafish swam along the social area throughout the experiment, whereas the *nomo1*$^{-/-}$ zebrafish swam in a dispersed and random manner. The heat map in Fig. 4B-C was obtained by analyzing the trajectory of the zebrafish in the mating tank. The ratio of time spent/distance moved in the social area was statistically significantly lower for *nomo1*$^{-/-}$ zebrafish than for *nomo1*$^{+/+}$ zebrafish (Fig. 4D-E). We used one of the videos to analyze the trajectory of the zebrafish. The shoaling behavior was detected to assess the social skills of WT and *nomo1*$^{-/-}$ zebrafish [32]. Generally, the group WT zebrafish swam together in an open-field test, reflecting the social nature of the species. The *nomo1*$^{-/-}$zebrafish showed an increased inter-individual distance with their companions than the *nomo1*$^{+/+}$ zebrafish, indicating that the *nomo1*$^{-/-}$zebrafish had a weaker clustering ability (Fig. 4G).

We also used videos to display the different types of repetitive behaviors of 2 mpf mutant zebrafish, including back-and-forth motion (Video S5), stereotypic movement (Video S6) and large circular movement (Video S7). The trajectories of the repetitive behaviors are shown in Fig. 4H. The numbers of different types of repetitive behaviors were counted. The mutant zebrafish exhibited more of these behaviors than the WT zebrafish and displayed a repetitive behavior-related pattern. The back-and-forth motion was significantly increased in mutant zebrafish compared to WT zebrafish (Fig. 4I). However, the number of stereotypic movements and large circular movements were not significantly different between *nomo1*$^{-/-}$ and WT zebrafish (Fig. 4I).

The WT zebrafish (Video S8) and *nomo1*$^{-/-}$ zebrafish (Video S9) displayed similar tendencies in kin preference region and non-kin preference region. The time spent/distance moved ratio of the mutant was the same as *nomo1*$^{+/+}$ zebrafish (Fig. S3B-C).

Loss-of-function of *nomo1* affected the midbrain and hindbrain during zebrafish development

At early stages, abundant *nomo1* mRNA is transcribed in the endoderm and anterior mesendoderm [9]. In our study, changes in the patterning of the endoderm marker *sox17* and mesoderm marker *hgg1* were detected in *nomo1*-deficient mutants. Loss-of-function of *nomo1* resulted in a different expression pattern of *hgg1* (Fig. 5A-B) (50% of cases, n=20). In our study, *nomo1* mutant embryos displayed an increased number of *sox17*-positive cells (Fig. 5C-D, arrows) (62% of cases, n=18).

Because *nomo1* is important for the development of the early mesendoderm, we examined various key neural development-related genes in WT and mutant zebrafish. The expression levels of the genes (*HuC, neurog1, islet1, egr2b* and *foxb1a*) in *nomo1* mutant zebrafish were not detectably different compared with the levels in WT zebrafish at 24 hpf (Fig. 5E), whereas the mRNA expression levels of the genes decreased significantly in the zebrafish at 48 hpf (Fig. 5F). We used RT-qPCR to detect the differences in expression levels in zebrafish, and then a semi-quantitative analysis was performed using WISH to verify the expression pattern. The *nomo1*$^{-/-}$ zebrafish exhibited significant differences in brain development compared with the WT, which was characterized by an absence of expression in midbrain and hindbrain at 48 hpf (Fig. 5G-L, arrows).

We performed HE staining of brain slices from adult zebrafish to determine whether the abnormalities in the brains of larval zebrafish persist throughout development (Fig. 5M-P). HE staining showed that the *nomo1*-deficient zebrafish had an abnormal brain structure during development. The changes were mainly manifested as loose and fragile brain tissue, and the midbrain and hindbrain regions of mutant zebrafish exhibited enlarged interstitial spaces. However, staining for forebrain-related markers, such as *fezf2*, and dopaminergic neurons did not reveal differences between WT and *nomo1*$^{-/-}$ larvae, indicating that the *nomo1* deficiency did not substantially alter forebrain and dopaminergic neuron development (Fig. S2). Based on the aforementioned microscopic morphology at the overall cellular level, we concluded that *nomo1* regulates early neural developmental patterning in vivo, strongly influencing the development of the midbrain and hindbrain in zebrafish.

Expression levels of neurotransmitters and metabolites were altered in the brains of juvenile *nomo1*$^{-/-}$ zebrafish

We examined neurotransmitters and metabolites in juvenile zebrafish brains to reveal the mechanism underlying the autism-like behaviors. Here, we focused on the following 13 neurotransmitters and their metabolites using the LC-MS/MS method: *r*-amino-butyric acid, levodopa, DA, epinephrine, 5-HIAA, serotonin, 3-methoxytyramine, acetylcholine, histamine, normetanephrine, tyramine, glutamate, and glutamine. Fig. 6A shows the cluster relationships of each metabolite between *nomo1*$^{+/+}$ and *nomo1*$^{-/-}$ zebrafish, and the tree structure at the left shows the clustering relationship of each group. The results of the hierarchical clustering analysis showed increased levels of ten neurotransmitters and their metabolites in *nomo1*$^{-/-}$ zebrafish compared with *nomo1*$^{+/+}$ zebrafish. Detailed descriptions of the quantities of the different metabolites are shown in Fig. 6B, and the expression of γ-aminobutyric acid, levodopa, epinephrine, serotonin, 3-methoxytyramine, histamine, normetanephrine, tyramine, glutamate, and glutamine was significantly higher in *nomo1*$^{-/-}$ zebrafish than in *nomo1*$^{+/+}$zebrafish.

Another method for detecting neurotransmitters, HPLC analysis, produced the same trend. In *nomo1*$^{-/-}$ zebrafish, the levels of serotonin and norepinephrine were obviously increased (Fig. 6C). Although the levels of dopamine and its metabolite DOPAC showed an increasing trend, the difference was not statistically significant (Fig. 6C).

The transcriptome analysis showed different gene expression patterns in the WT and mutant zebrafish

The juvenile zebrafish were selected for the transcriptome sequencing analysis to further study the functional mechanism between ASD-like phenotypes and *nomo1* deficiency at the genetic level. A volcano map visually shows the distributions of DEGs for each of the comparisons. Two hundred ninety-two genes were downregulated, 254 genes were upregulated, and the expression of 546 genes was changed at the transcriptional level in mutant zebrafish (Fig. 7A). The altered DEGs are listed and their p-values are shown in Table S2. We performed GO annotation and KEGG pathway analyses to understand the functions and roles of DEGs. The GO annotation classification chart revealed the functions of DEGs in biological processes, cellular components and molecular functions (Fig. 7B). Through the classification and statistical analysis of KEGG signaling pathways, *nomo1* was shown to participate in the biological processes of metabolism, cellular function, intestinal immunity, and pathogen infection (Fig. 7C).

A functional analysis of the DEGs revealed that *nos2a* and *hbba1* were upregulated, whereas *rnps1*, *ass1*, s*lc39a8*, *slc43a2b*, *cfap100*, *slc15a2* and *entpd8* were downregulated in mutant zebrafish compared to their expression in WT zebrafish. RT-qPCR was used to verify the mRNA expression levels of DEGs and confirmed that the difference in gene expression was consistent with the sequencing results (Fig. 7D).

The decreased locomotion of 7 dpf zebrafish was recovered by the neuroactive drug PTZ

We applied the neuroactive drug PTZ, an antagonist of the γ-aminobutyrate (GABA) receptor, and measured the locomotor activity of larval zebrafish to explore the effects of drugs that alter neurological disease-related phenotypes. Here, 8 mM PTZ was utilized. The experiment lasted for 60 min and was conducted under continuous illumination. The zebrafish were maintained in a 24-well plate at a room temperature of 28°C room. The movement trajectories of zebrafish (*nomo1*$^{+/+}$, *nomo1*$^{-/-}$, *nomo1*$^{+/+}$+PTZ, and *nomo1*$^{-/-}$+PTZ) in the experimental period are shown in Fig. 2I. Upon exposure to PTZ, WT zebrafish exhibited increased locomotion, similar to our previous study [20]. The locomotor activity of mutant zebrafish treated with PTZ increased significantly compared with *nomo1*$^{-/-}$ zebrafish, and a statistically significant difference in locomotor activity was observed under continuous illumination conditions (Fig. 2J).

Discussion

Although some functional roles of *nomo1* have been described in previous studies, the effects of neuropsychiatric system caused by *nomo1* deficiency remain unclear. In this study, we reported the morphological, behavioral and functional mechanism of *nomo1* mutant zebrafish at different developmental stages. Previous *nomo1* KO zebrafish model that was associated with bone formation and cartilage development [13]. Authors observed early-stage bone developmental defects in larvae before 7 dpf, which might be one of reasons for the behavioral disorders in larval and infant zebrafish. Behavioral features are influenced by many factors, particularly in context of the neuropsychiatric system

and motor ability. Although the change of locomotor activity is difficult to estimate from the nervous system or bone developmental defects, the social-level results make sense, emphasizing the importance of *nomo1* in neuropsychiatric systems. The locomotion of juvenile mutant zebrafish did not change compared with WT zebrafish; however, the specific movement pattern did change. Based on the abundance of *nomo1* throughout the brain, we consider that the overall fiber morphology of the brain might have changed due to the mutation, subsequently influencing the nervous system to affect the behavioral phenotype. Thus, *nomo1* loss-of-function exerted an important effect on the neuropsychiatric system in zebrafish.

Our study provides several important findings. We highlight the essential role of *nomo1* in ASD-like phenotypes during development. Behavioral assays of *nomo1* mutant zebrafish in the juvenile period presented social defects and repetitive behaviors, which is similar with autism-like behaviors. Similar phenotypes have been observed in other transgenic mutant zebrafish models of *shank3b* [22], *dyrk1a* [25] and *fmr1* [33]. Here, we analysed our results by comparing them with findings from studies that used zebrafish to investigate the function of genes that are strongly associated with ASD (Table S3). Combined with clinical research, our results show the functional deficiency of *nomo1* as an underlying disease mechanism for autism. Autism is one of the neuropsychiatric disorders, and comorbidities are common in patients [18, 34]. Developing *nomo1* mutant zebrafish exhibited decreased/increased locomotion, speculating the mutant zebrafish not only displayed autism-like behavior but also related to ADHD- or epilepsy-like phenotypes. However, further studies are warranted to determine whether the behavioral phenotype observed in animal models is directly associated with human diseases. Neuropsychiatric disorders exhibit substantial heterogeneity. Different gene mutations may lead to a specific disease, and a single gene mutation can cause comorbidities in individuals with ASD and other neuropsychiatric diseases. Therefore, studies of the functions of different genes, different signaling pathways and different mutation models are warranted to determine the pathogenesis of the diseases. Moreover, additional behavioral measurements, including comorbidities such as seizures and cognitive impairment, are needed to fully assess neuropsychiatric disease-like behavioral phenotypes using validate animal model.

Based on our results, the loss-of-function of *nomo1* influenced the development of the midbrain and hindbrain. Haffner *et al.* indicated that transiently decreased expression of *nomo1* affects the development of the mesendoderm and hatching glands [9]. Specifically, our study revealed abnormal expression levels of mesendoderm and endodermal markers in steadily inherited embryonic mutant zebrafish. The potential neural induction properties of the mesendoderm indicate that the mesendoderm is necessary for brain development [35, 36]. Meanwhile, we detected abnormalities in brain developmental markers during the early neural development of mutant larvae accompanied by loosening of the tissue structure in the midbrain and hindbrain of adult mutant zebrafish. Patients with ASD exhibit a reduced brain parenchyma in magnetic resonance imaging (MRI) [37]. Thus, our findings also provided a logical consistency between structural abnormalities in the brain and behavioral phenotypes related to ASD. Moreover, researchers have indicated that *nomo1* affects body axis development [9], which might be the cause of the increased mortality and varying degrees of developmental malformations observed in

larval zebrafish in this study. Notably, the delayed neurodevelopment in terms of the appearance of the phenotype and body length in mutant zebrafish became less noticeable during development. The mechanism underlying this effect is currently unknown, but *nomo1* can affect morphological development at specific stage to exert a more pronounced effect on the nervous system across developmental stages.

Behavioral phenotypes are associated with a complex pathogenesis, which is typically characterized by alterations in the activity of neurotransmitters. Genetic association studies have verified the key role of DA in the etiology of ADHD [38, 39]. In our study, targeted metabolomics showed a significant increase in the levels of levodopa, a precursor of DA. However, the level of the metabolite DA had not changed in mutant zebrafish compared to WT zebrafish, as determined using HPLC. This result is consistent with the changes in dopamine neurons observed in larvae zebrafish using WISH. We speculated that other precursors of DA collectively modulated the level of DA. Interestingly, we detected alterations in γ-aminobutyrate (GABA), glutamate and serotonin levels when analyzing neurotransmitter metabolism. Moreover, 5-HT was shown to accumulate at a high rate using both of these methods. Evidence supports a novel and important link between schizophrenia, GABA and glutamate alterations [40]. In addition, several findings suggest a correlation between glutamate and GABA in subjects with ASD, which also indicated that the neurotransmitter contributed to brain development [41, 42]. Abnormalities in the neurotransmitter system have been observed in children or animal models with neuropsychiatric disorders, involving mainly glutamatergic, GABAergic and other neuronal populations [43, 44]. Clinical studies have documented elevated levels of 5-HT in the peripheral blood of children with ASD [45], and some researchers have reported differences in the 5-HT distribution in different regions of the brains of patients with ASD [46]. Therefore, we concluded that the *nomo1* deficiency displayed a strong correlation with brain metabolism of GABA, glutamate and 5-HT in zebrafish, which represent a vital decision-making aspect of autism-like behavior. However, the mechanism of how neurotransmitters affect behavioral changes is unclear. In future studies, metabolism mechanism and pathway of neurotransmitters in brain involved in *nomo1* KO zebrafish model will be examined.

Transcriptome sequencing analyses have identified multiple DEGs associated with neuropsychiatric disorders. For example, the association of *RNPS1* and *NOS2* with neurodevelopmental disorders in patients has been verified [47, 48]. Additionally, researchers have presented evidences strongly suggesting and association between *SLC39A8* and schizophrenia [49]. We also identified other DEGs with abnormal expression levels in mutant zebrafish (*ass1, hbba1, slc43a2b, cfap100*, *entpd8*, and *slc15a2*). Some of these genes are novel, and their functions have not been completely elucidated in the neuropsychiatric system. However, the DEGs may provide important clues regarding the neuropsychiatric disorders observed due to a *nomo1* deficiency at the genetic level. Although our study was limited, the transcriptome results provided clues for studying the interaction network between genes. Moreover, it will provide new directions for studies of the signaling pathways associated with DEGs correlated with *nomo1* deficiency with neuropsychiatric system.

The analysis of neurotransmitter metabolism revealed that *nomo1* is associated with GABA signaling in zebrafish. GABA is an inhibitory neurotransmitter of the central nervous system, and PTZ is an antagonist of the GABA receptor. Therefore, we attempted to reverse part of the behavioral phenotypes in the *nomo1* mutant zebrafish model using PTZ. PTZ increased the spontaneous movement of larval zebrafish under light conditions [20]. In addition, Mussulini *et al.* found that an increase in the PTZ concentration increased body movement and seizure-like behavior, which were observed following treatment with 15 mM PTZ in adult zebrafish [50]. In the present study, we inferred that mutant zebrafish remained sensitive to neuroactive drugs and that PTZ partially improved the locomotor activity of larval mutant zebrafish. The ASD include a range of characteristic behavioral phenotypes, whereas the exploration of therapeutic effects of targeted small-molecule compounds obviously require further research. This study provides a powerful functional basis for the future exploration of drug sensitivity and intervention in *nomo1* mutant zebrafish and may provide additional insights into research performed on this topic in the future.

Taken together, the data presented here conclusively indicate that *nomo1* deficiency causes abnormal development of the nervous system and autism-like behaviors in zebrafish. The *nomo1* zebrafish model described in this study provides an important foundation for neuroactive drug screens in precision medicine in the future.

Limitations

As shown in the present study, the loss-of-function of *nomo1* elicits autism-like behaviors; however, more evidence on molecular pathogenic mechanisms of *nomo1* deficiency is needed. Moreover, the effects of an intervention with a neuroactive drug on the behavioral phenotype and functional mechanism of mutant zebrafish requires additional detailed and extensive evidence.

Conclusions

In this study, we generated a *nomo1* loss-of-function zebrafish model that presented autism-like phenotypes, particularly social defects and repetitive behaviors in juvenile zebrafish. The enlarged interstitial spaces of midbrain and hindbrain in *nomo1*$^{-/-}$ zebrafish suggest the functional mechanism of *nomo1* deficiency in brain development. The increased neurotransmitter levels of γ-aminobutyrate, glutamate and serotonin in *nomo1*$^{-/-}$ zebrafish and transcriptome analysis at the genetic level also provide further evidence supporting the potential role of *nomo1* deficiency resulted in autism-like phenotypes. These results indicate a functional deficiency of *nomo1* as a candidate gene for autism. The *nomo1* mutant zebrafish provide a valuable model for future studies of the molecular pathogenesis of *nomo1*-related disorders and drug screening.

Declarations

Acknowledgments

We thank all members of the Qiang Li laboratory for their support, and we thank the Translational Medical Center for Development and Disease of Children's Hospital of Fudan University in China. We thank Dr. Ning Guo for the advice on behavioral analyses and Chenwen Zhu for technical discussions related to the experiments.

Funding

This study was supported by grants from the National Natural Science Foundation of China (NSFC, no. 81771632 and no. 81271509) to Qiang Li. Xiuyun Liu is supported by a grant from the NSFC (no. 81601329).

Availability of data and materials

The datasets analyzed in the current study are available from the corresponding author upon reasonable request.

Authors' contributions

This study was designed by QL, XW and FL. FL, JL, TTL and JJ performed the experiments. FL wrote the manuscript, with extensive editing by QL. YLZ, XYL and YXJ designed the CRISPR/Cas9-mediated mutagenesis of *nomo1* loci in zebrafish and provided assistance with the identification of homozygous animals. QZ provided technical assistance with transcriptomics and HPLC analyses. All authors read and approved the final manuscript.

Ethical approval

All procedures were approved by the Institutional Animal Care Committee of Children's Hospital of Fudan University, China.

Competing interests

The authors declare no conflicts of interest.

Consent for publication

Not applicable.

Abbreviations

ASD: autism spectrum disorder, ADHD: attention deficit hyperactivity disorder, CNVs: copy number variations, WISH: whole-mount in situ hybridization, PTZ: pentylenetetrazole, dpf: days postfertilization, mpf: months postfertilization, SgRNA: specific guide RNA, RT-qPCR: real-time quantitative polymerase chain reaction, LC-MS/MS: liquid chromatography-tandem mass spectrometry, HPLC: high-performance

liquid chromatography, HE staining: hematoxylin-eosin staining, DEGs: differentially expressed genes, WT: wild-type, PMS: Phelan-McDermid syndrome.

References

1. Mefford, H.C., et al., *Genome-wide copy number variation in epilepsy: novel susceptibility loci in idiopathic generalized and focal epilepsies.* PLoS Genet, 2010. **6**(5): p. e1000962.
2. Williams, N.M., et al., *Rare chromosomal deletions and duplications in attention-deficit hyperactivity disorder: a genome-wide analysis.* Lancet, 2010. **376**(9750): p. 1401-8.
3. Akahoshi, K., et al., *A woman with 46,XX,dup(16)(p13.11 p13.3) and the ATR-X phenotype.* Am J Med Genet A, 2005. **132A**(4): p. 414-8.
4. Ramalingam, A., et al., *16p13.11 duplication is a risk factor for a wide spectrum of neuropsychiatric disorders.* J Hum Genet, 2011. **56**(7): p. 541-4.
5. Tassano, E., et al., *Concomitant deletion of chromosome 16p13.11 and triplication of chromosome 19p13.3 in a child with developmental disorders, intellectual disability, and epilepsy.* Mol Cytogenet, 2015. **8**: p. 9.
6. Brownstein, C.A., et al., *Overlapping 16p13.11 deletion and gain of copies variations associated with childhood onset psychosis include genes with mechanistic implications for autism associated pathways: Two case reports.* Am J Med Genet A, 2016. **170A**(5): p. 1165-73.
7. Dettmer, U., et al., *Transmembrane protein 147 (TMEM147) is a novel component of the Nicalin-NOMO protein complex.* J Biol Chem, 2010. **285**(34): p. 26174-81.
8. Haffner, C., et al., *The Nicastrin-like protein Nicalin regulates assembly and stability of the Nicalin-nodal modulator (NOMO) membrane protein complex.* J Biol Chem, 2007. **282**(14): p. 10632-8.
9. Haffner, C., et al., *Nicalin and its binding partner Nomo are novel Nodal signaling antagonists.* EMBO J, 2004. **23**(15): p. 3041-50.
10. Huang, Y.T., et al., *Genotype-based gene signature of glioma risk.* Neuro Oncol, 2017. **19**(7): p. 940-950.
11. Perea, J., et al., *NOMO-1 gene is deleted in early-onset colorectal cancer.* Oncotarget, 2017. **8**(15): p. 24429-24436.
12. Nicot, R., et al., *Nodal pathway genes are down-regulated in facial asymmetry.* J Craniofac Surg, 2014. **25**(6): p. e548-55.
13. Cao, L., et al., *Loss of the Nodal modulator Nomo results in chondrodysplasia in zebrafish.* Curr Mol Med, 2018. **18**(7): p. 448-458.
14. Lahey, B.B. and E.G. Willcutt, *Predictive validity of a continuous alternative to nominal subtypes of attention-deficit/hyperactivity disorder for DSM-V.* J Clin Child Adolesc Psychol, 2010. **39**(6): p. 761-75.
15. Gnanavel, S. and R.S. Robert, *Diagnostic and statistical manual of mental disorders, fifth edition, and the impact of events scale-revised.* Chest, 2013. **144**(6): p. 1974.

16. Christensen, D.L., et al., *Prevalence and Characteristics of Autism Spectrum Disorder Among Children Aged 8 Years--Autism and Developmental Disabilities Monitoring Network, 11 Sites, United States, 2012.* MMWR Surveill Summ, 2016. **65**(3): p. 1-23.
17. Chaste, P. and M. Leboyer, *Autism risk factors: genes, environment, and gene-environment interactions.* Dialogues Clin Neurosci, 2012. **14**(3): p. 281-92.
18. Subramanian, D., et al., *Gamma oscillatory activity in vitro: a model system to assess pathophysiological mechanisms of comorbidity between autism and epilepsy.* Transl Psychiatry, 2018. **8**(1): p. 16.
19. Chou, I.C., et al., *Correlation between epilepsy and attention deficit hyperactivity disorder: a population-based cohort study.* PLoS One, 2013. **8**(3): p. e57926.
20. Peng, X.L., et al., *Anxiety-related behavioral responses of pentylenetetrazole-treated zebrafish larvae to light-dark transitions.* Pharmacology Biochemistry And Behavior, 2016. **145**: p. 55-65.
21. Blaser, R. and R. Gerlai, *Behavioral phenotyping in zebrafish: comparison of three behavioral quantification methods.* Behav Res Methods, 2006. **38**(3): p. 456-69.
22. Liu, C.X., et al., *CRISPR/Cas9-induced shank3b mutant zebrafish display autism-like behaviors.* Mol Autism, 2018. **9**: p. 23.
23. Gong, J., et al., *Insm1a Regulates Motor Neuron Development in Zebrafish.* Front Mol Neurosci, 2017. **10**: p. 274.
24. Schwarzer, S., et al., *Dlx3b/4b is required for early-born but not later-forming sensory hair cells during zebrafish inner ear development.* Biol Open, 2017. **6**(9): p. 1270-1278.
25. Kim, O.H., et al., *Zebrafish knockout of Down syndrome gene, DYRK1A, shows social impairments relevant to autism.* Mol Autism, 2017. **8**: p. 50.
26. Mali, P., et al., *RNA-guided human genome engineering via Cas9.* Science, 2013. **339**(6121): p. 823-6.
27. Hwang, W.Y., et al., *Efficient genome editing in zebrafish using a CRISPR-Cas system.* Nat Biotechnol, 2013. **31**(3): p. 227-9.
28. Miller, N.Y. and R. Gerlai, *Shoaling in zebrafish: what we don't know.* Rev Neurosci, 2011. **22**(1): p. 17-25.
29. Huang, F., et al., *Simultaneous quantification of seven hippocampal neurotransmitters in depression mice by LC-MS/MS.* J Neurosci Methods, 2014. **229**: p. 8-14.
30. Santos-Fandila, A., et al., *Analysis of 17 neurotransmitters, metabolites and precursors in zebrafish through the life cycle using ultrahigh performance liquid chromatography-tandem mass spectrometry.* J Chromatogr B Analyt Technol Biomed Life Sci, 2015. **1001**: p. 191-201.
31. Bloom, L. and V. Calabro, *FN3: a new protein scaffold reaches the clinic.* Drug Discov Today, 2009. **14**(19-20): p. 949-55.
32. Buske, C. and R. Gerlai, *Maturation of shoaling behavior is accompanied by changes in the dopaminergic and serotoninergic systems in zebrafish.* Dev Psychobiol, 2012. **54**(1): p. 28-35.

33. Kim, L., et al., *Anxiety, hyperactivity and stereotypy in a zebrafish model of fragile X syndrome and autism spectrum disorder.* Prog Neuropsychopharmacol Biol Psychiatry, 2014. **55**: p. 40-9.
34. Salazar, F., et al., *Co-occurring Psychiatric Disorders in Preschool and Elementary School-Aged Children with Autism Spectrum Disorder.* J Autism Dev Disord, 2015. **45**(8): p. 2283-94.
35. Acampora, D., et al., *Forebrain and midbrain regions are deleted in Otx2-/- mutants due to a defective anterior neuroectoderm specification during gastrulation.* Development, 1995. **121**(10): p. 3279-90.
36. Camus, A., et al., *The morphogenetic role of midline mesendoderm and ectoderm in the development of the forebrain and the midbrain of the mouse embryo.* Development, 2000. **127**(9): p. 1799-813.
37. Turner, A.H., K.S. Greenspan, and T.G.M. van Erp, *Pallidum and lateral ventricle volume enlargement in autism spectrum disorder.* Psychiatry Res Neuroimaging, 2016. **252**: p. 40-45.
38. LaHoste, G.J., et al., *Dopamine D4 receptor gene polymorphism is associated with attention deficit hyperactivity disorder.* Mol Psychiatry, 1996. **1**(2): p. 121-4.
39. Lange, M., et al., *The ADHD-susceptibility gene lphn3.1 modulates dopaminergic neuron formation and locomotor activity during zebrafish development.* Mol Psychiatry, 2012. **17**(9): p. 946-54.
40. Lewis, D.A. and B. Moghaddam, *Cognitive dysfunction in schizophrenia: convergence of gamma-aminobutyric acid and glutamate alterations.* Arch Neurol, 2006. **63**(10): p. 1372-6.
41. Fatemi, S.H., et al., *Downregulation of GABAA receptor protein subunits alpha6, beta2, delta, epsilon, gamma2, theta, and rho2 in superior frontal cortex of subjects with autism.* J Autism Dev Disord, 2014. **44**(8): p. 1833-45.
42. Lam, K.S., M.G. Aman, and L.E. Arnold, *Neurochemical correlates of autistic disorder: a review of the literature.* Res Dev Disabil, 2006. **27**(3): p. 254-89.
43. Ang, G., et al., *Absent sleep EEG spindle activity in GluA1 (Gria1) knockout mice: relevance to neuropsychiatric disorders.* Transl Psychiatry, 2018. **8**(1): p. 154.
44. Sapey-Triomphe, L.A., et al., *Tactile hypersensitivity and GABA concentration in the sensorimotor cortex of adults with autism.* Autism Res, 2019. **12**(4): p. 562-575.
45. Anderson, G.M., et al., *Whole blood serotonin in autistic and normal subjects.* J Child Psychol Psychiatry, 1987. **28**(6): p. 885-900.
46. Chugani, D.C., et al., *Altered serotonin synthesis in the dentatothalamocortical pathway in autistic boys.* Ann Neurol, 1997. **42**(4): p. 666-9.
47. Nguyen, L.S., et al., *Contribution of copy number variants involving nonsense-mediated mRNA decay pathway genes to neuro-developmental disorders.* Hum Mol Genet, 2013. **22**(9): p. 1816-25.
48. Kim, H.W., et al., *Family-based association study between NOS-I and -IIA polymorphisms and autism spectrum disorders in Korean trios.* Am J Med Genet B Neuropsychiatr Genet, 2009. **150B**(2): p. 300-6.
49. Costas, J., *The highly pleiotropic gene SLC39A8 as an opportunity to gain insight into the molecular pathogenesis of schizophrenia.* American Journal of Medical Genetics Part B-Neuropsychiatric Genetics, 2018. **177**(2): p. 274-283.

50. Mussulini, B.H., et al., *Seizures induced by pentylenetetrazole in the adult zebrafish: a detailed behavioral characterization.* PLoS One, 2013. **8**(1): p. e54515.

Figures

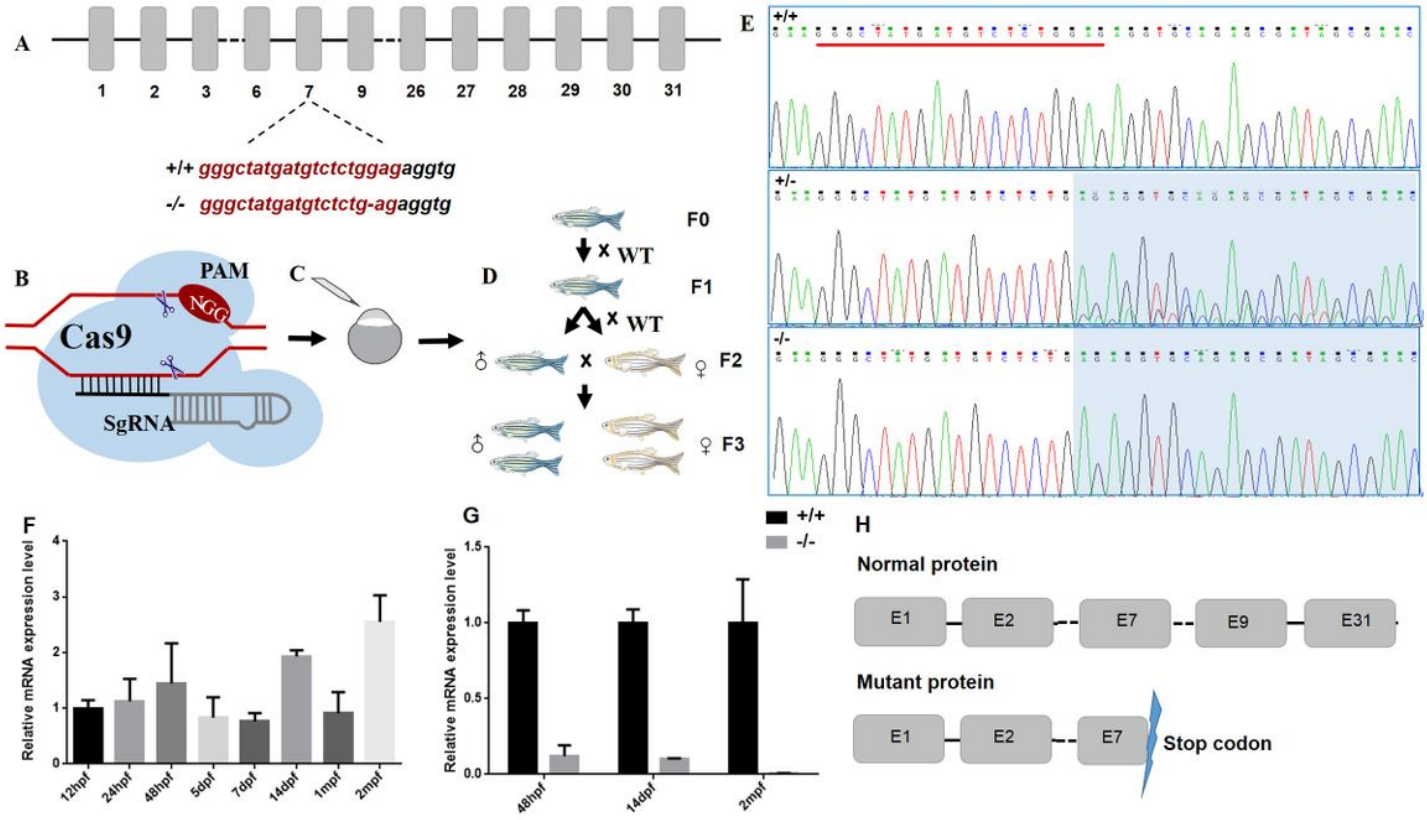

Figure 1

The expression level of the nomo1 mRNA during development and generation of hereditary nomo1 mutant zebrafish. (A) Structure of the zebrafish nomo1 gene. Exon 7 was the target site in zebrafish. (B) The principle of the CRISPR/Cas9 technique. (C) Microinjection of zebrafish at the single-cell phase. (D) Acquisition of stable inherited homozygous zebrafish. (E) Sequencing results for nomo1 in WT, heterozygous and homozygous zebrafish. The mutation induced by CRISPR/Cas9 (1-base deletion) is shown in nomo1 mutant sequences. (F) The relative levels of the nomo1 transcript at different developmental stages. (G) Abnormal expression of the nomo1 mRNA in the whole embryo at 48 hpf, heads at 14 dpf and brain tissues at 2 mpf of nomo1-/- zebrafish analyzed using RT-qPCR. (H) Translation of the amino acids predicting the termination codon. Data are presented as the means ± SEM.

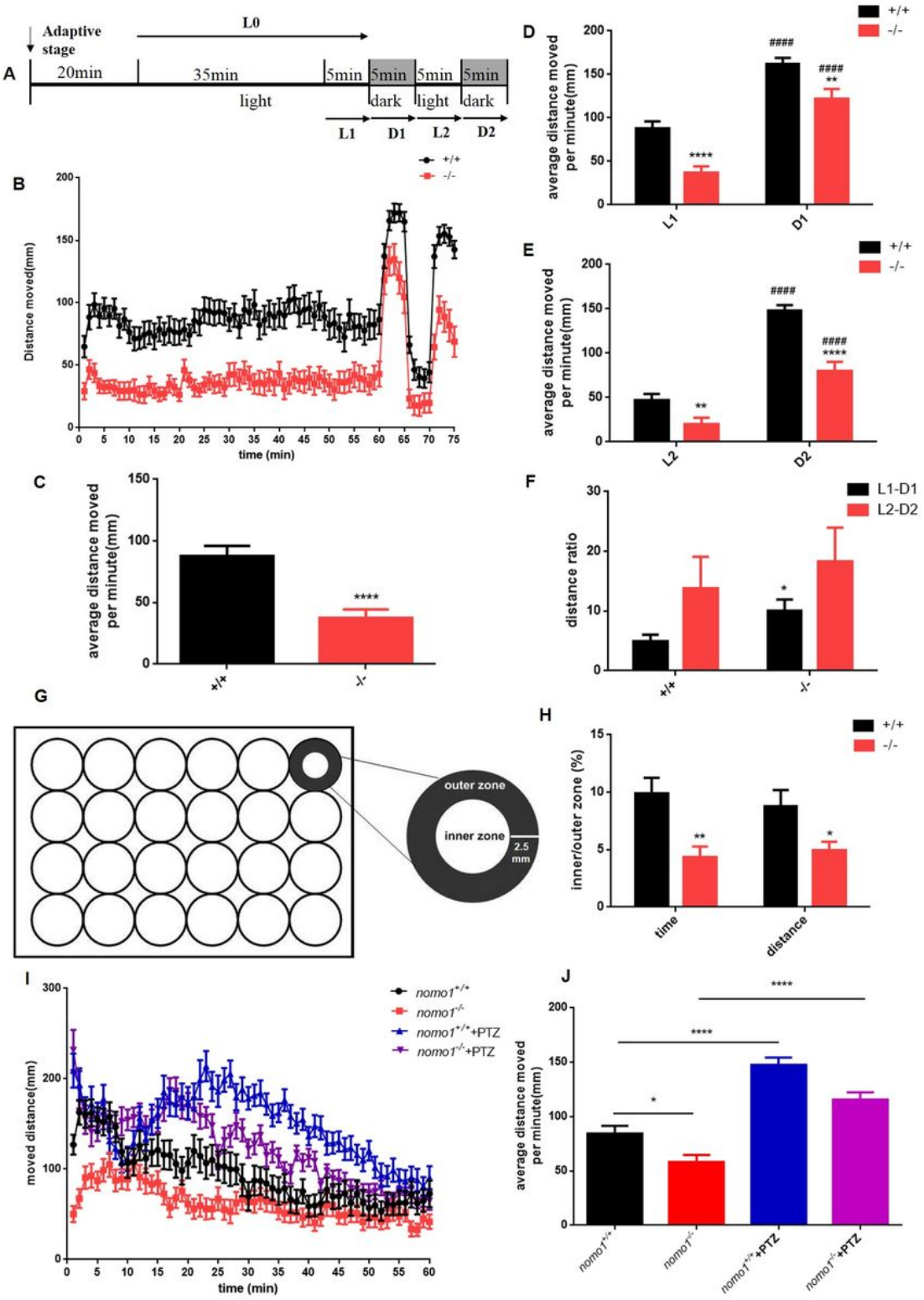

Figure 2

The locomotion of 7 dpf zebrafish treated with or without PTZ, and the thigmotaxis behavior of WT and mutant zebrafish. (A) Light/dark test of larval nomo1+/+ and nomo1-/- zebrafish at 7 dpf. The experiment lasted for 75 min and consisted of 40 min of light (L0) and two 5-min light/dark cycles (L1-D1 and L2-D2). (B) Trend for the total distances swum by larval zebrafish during the experimental period. The horizontal axis is the swimming time, and the vertical axis is the distance moved, which is used to

intuitively display the locomotion of the zebrafish over the experimental period. (C) The average distance moved within each 1-min bin under continuous illumination is shown (N = 48 zebrafish of each genotype). (D-E) The average distance moved per minute under two light/dark cycles is exhibited. * indicates a comparison with the WT group under the same lighting conditions. # indicates the same zebrafish under different illumination conditions. (F) The ratio of the distance moved by larval zebrafish during each light/dark cycle. (G) The testing apparatus in a 24-well plate. The inner and outer zones were delineated as shown above. The ratio of distance moved/time spent in the inner zone indicates thigmotaxis behavior. (H) The ratio of distance moved/time spent in the inner zone under light conditions (L0 period) in 7 dpf zebrafish larvae. (I-J) The decreased locomotion of nomo1-/- larval zebrafish was improved by PTZ (N = 36 for each genotype). (I) The trend in the total distance swum by 7 dpf larval zebrafish during 60 min of continuous illumination. (J) The average distance moved within each 1-min bin under continuous illumination is plotted. Data are presented as the means ± SEM, *p < 0.05, **p < 0.01, ****p < 0.0001, and ####p < 0.0001.

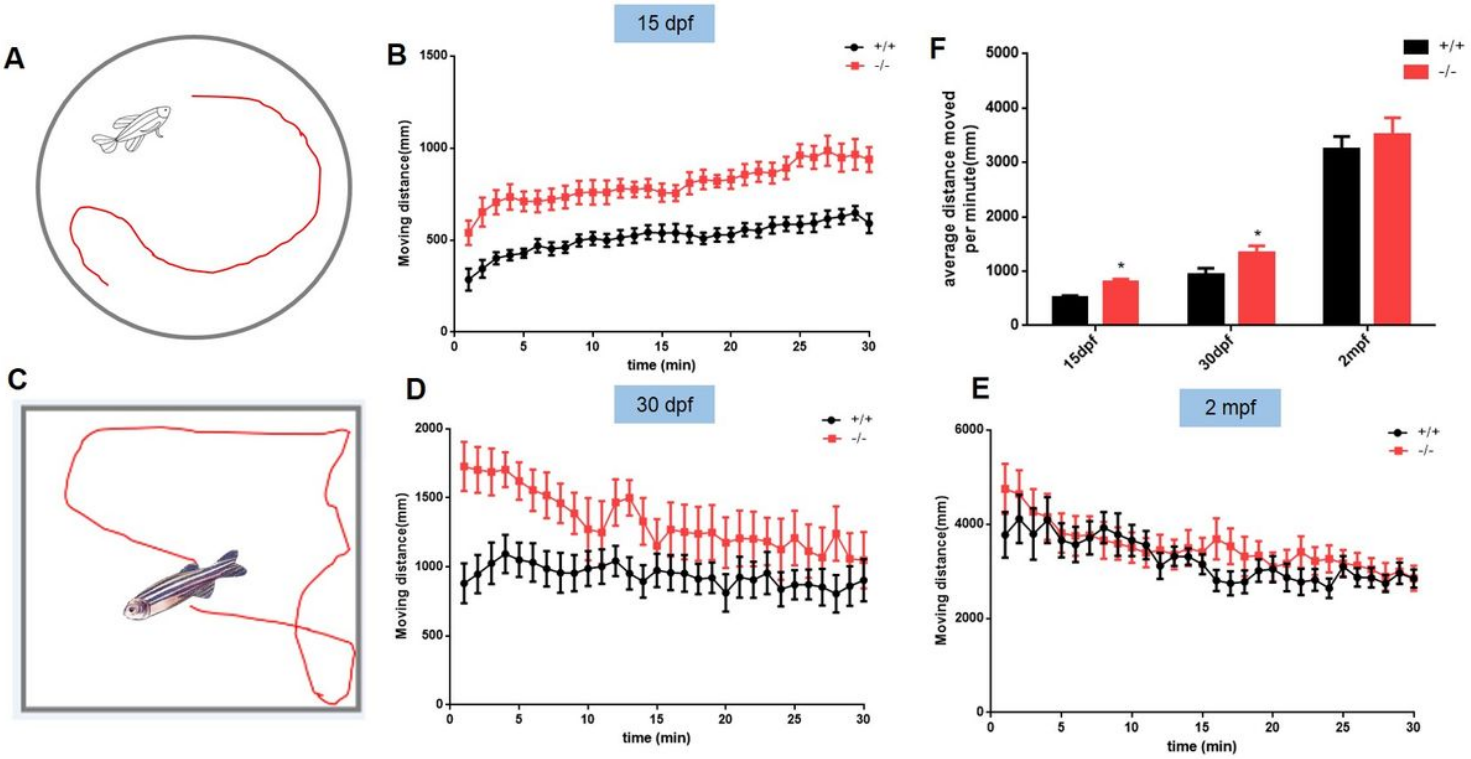

Figure 3

The locomotion of infant and juvenile WT and nomo1-/- zebrafish. (A) Container of 15 dpf zebrafish in the open field experiment. (C) Container of 30 dpf and 2 mpf zebrafish in the open field experiment. (B, D, and E) The locomotion of WT and mutant zebrafish over the total 30-min experimental period (N = 16 for each genotype at different developmental stages). (F) The average distance moved within each 1-min bin under continuous illumination is plotted. Data are presented as the means ± SEM, *p < 0.05.

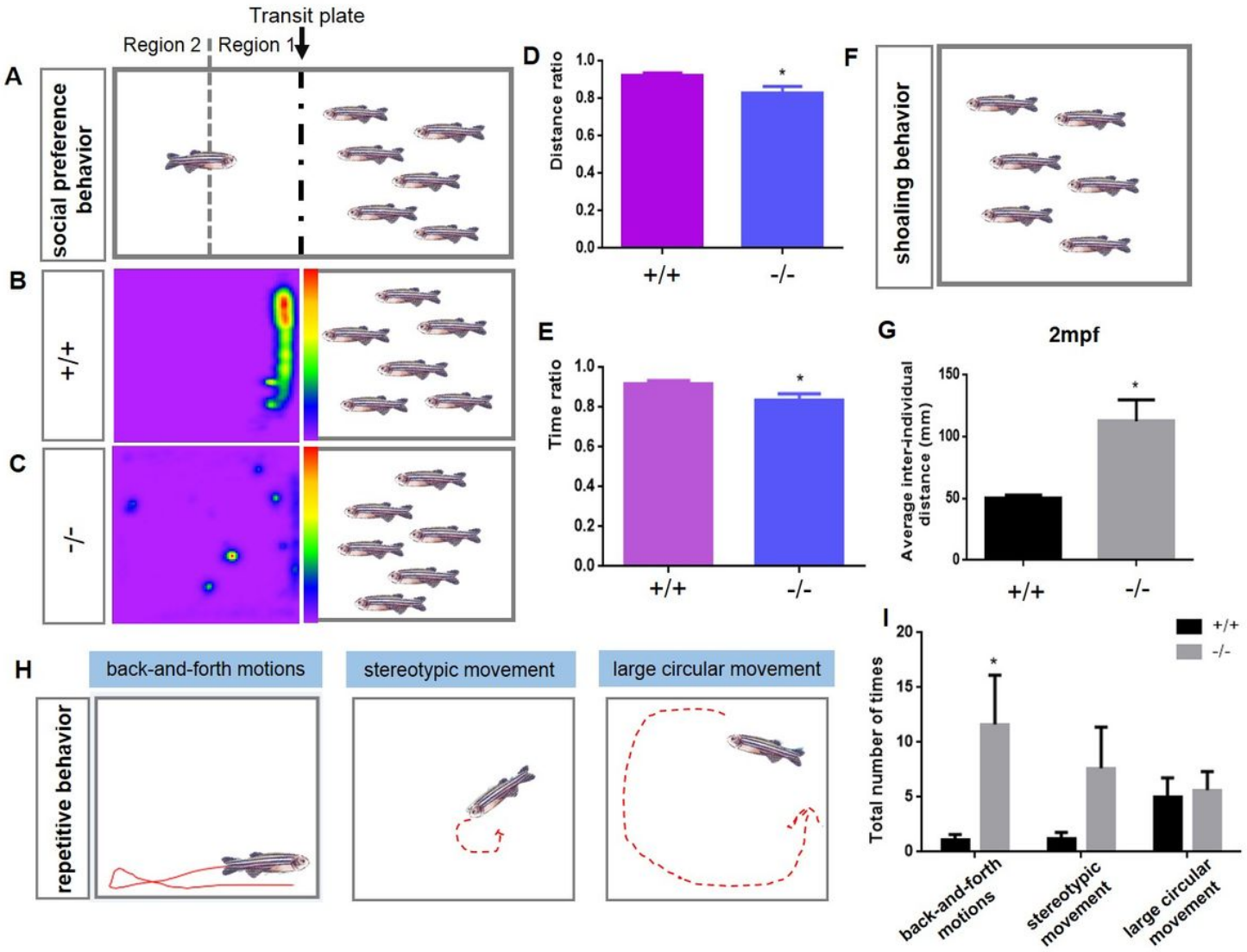

Figure 4

Juvenile nomo1-/- zebrafish displayed social deficiency and repetitive behaviors. (A-E) The social preference experiment with juvenile zebrafish. (A) Schematic diagram of the individual social behavior experiment. A heat map (B-C) showing that nomo1-/- zebrafish spent significantly less time in the social area than WT zebrafish. The ratio of distance from the social area (D) and time spent in the social area (E) was significantly lower for nomo1-/- zebrafish than for WT zebrafish (N = 20 zebrafish per group). Schematic of the shoaling test (F-G) in which the inter-individual distance exhibited by nomo1-/- zebrafish was significantly higher than WT zebrafish (N = 6×8 zebrafish per group). (H-I) Schematic of different representative behaviors shown by juvenile nomo1-/- zebrafish: including “back-and-forth motions”, “large circular movement” and “stereotypic movement”. Nomo1-/- zebrafish exhibited a significantly higher proportion of back-and-forth motions than nomo1+/+ zebrafish (N = 16 zebrafish per group). Data are presented as the mean ± SEM, *p < 0.05.

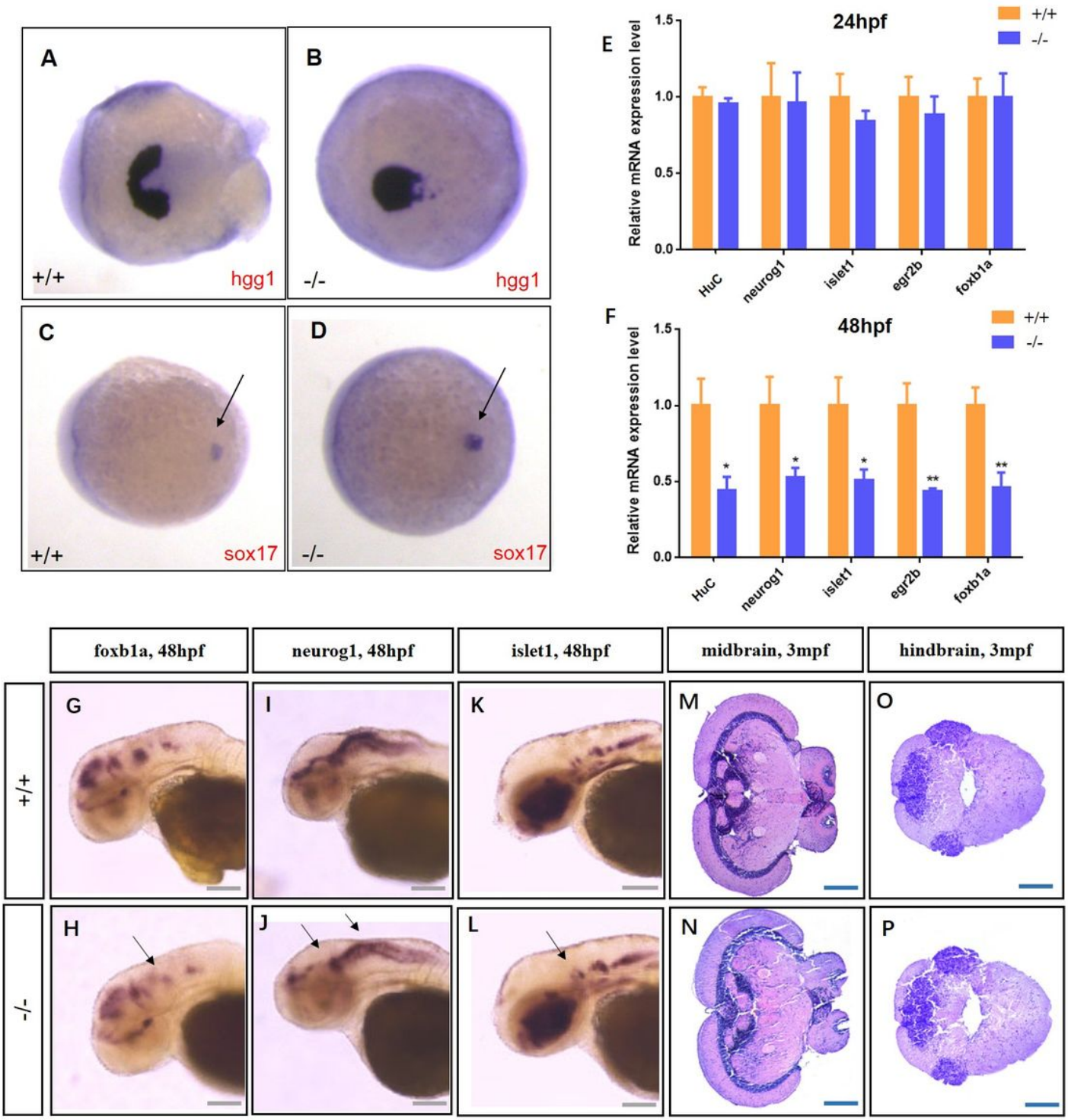

Figure 5

Loss-of-function of nomo1 affected neurodevelopment in larval zebrafish and in the brains of adult male zebrafish. (A-D) The sites of hgg1 and sox17 expression in WT and mutant zebrafish at 12 hpf determined using WISH. (E-F) The expression of neurological genes (HuC, neurog1, islet1, egr2b and foxb1a) in nomo1-/- zebrafish at 24 hpf and 48 hpf determined using RT-qPCR (N = 6×10 animals per group). Data are presented as the means ± SEM. *p < 0.05 and **p < 0.01. (G-L) Mutant zebrafish were

analyzed at 48 hpf using WISH to detect foxb1a (G-H), neurog1 (I-J) and islet1 (K-L) expression. The loss-of-function of nomo1 reduced the midbrain and hindbrain volumes in zebrafish at 48 hpf (arrows in H, J, and L; scale bar: 100 μm). (M-P) The midbrain and hindbrain structures of adult WT and mutant zebrafish (scale bar: 200 μm).

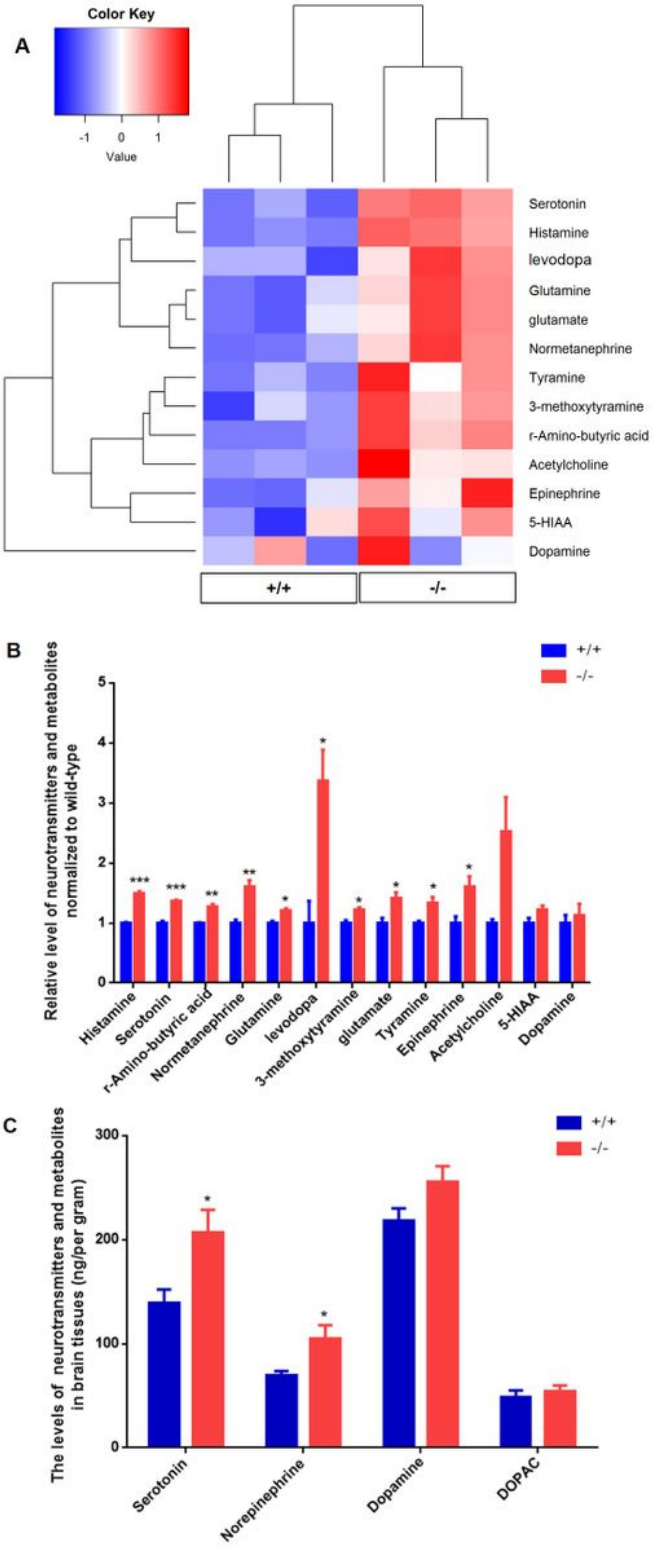

Figure 6

Differences in the expression of neurotransmitters and metabolites between the brain tissues of WT and nomo1-/- juvenile zebrafish. Thirteen neurotransmitters and metabolites were analyzed using the LC-MS/MS, and four neurotransmitters were analyzed using HPLC. (A) The clustering analysis of nomo1+/+ and nomo1-/- zebrafish using SRM/MRM revealed that neurotransmitters and metabolites tended to be upregulated in mutant zebrafish. (B) Statistical analysis of the SRM/MRM data. The vertical axis denotes the normalized levels of neurotransmitters and metabolites (N=3×8 groups each of WT and mutant zebrafish). (C) Statistical analysis of the HPLC data. The vertical axis denotes the levels of 4 neurotransmitters and metabolites in zebrafish brain tissues (N=8×7 for each group). Data are presented as the means±SEM, *p < 0.05, **p < 0.01, and ***p < 0.001.

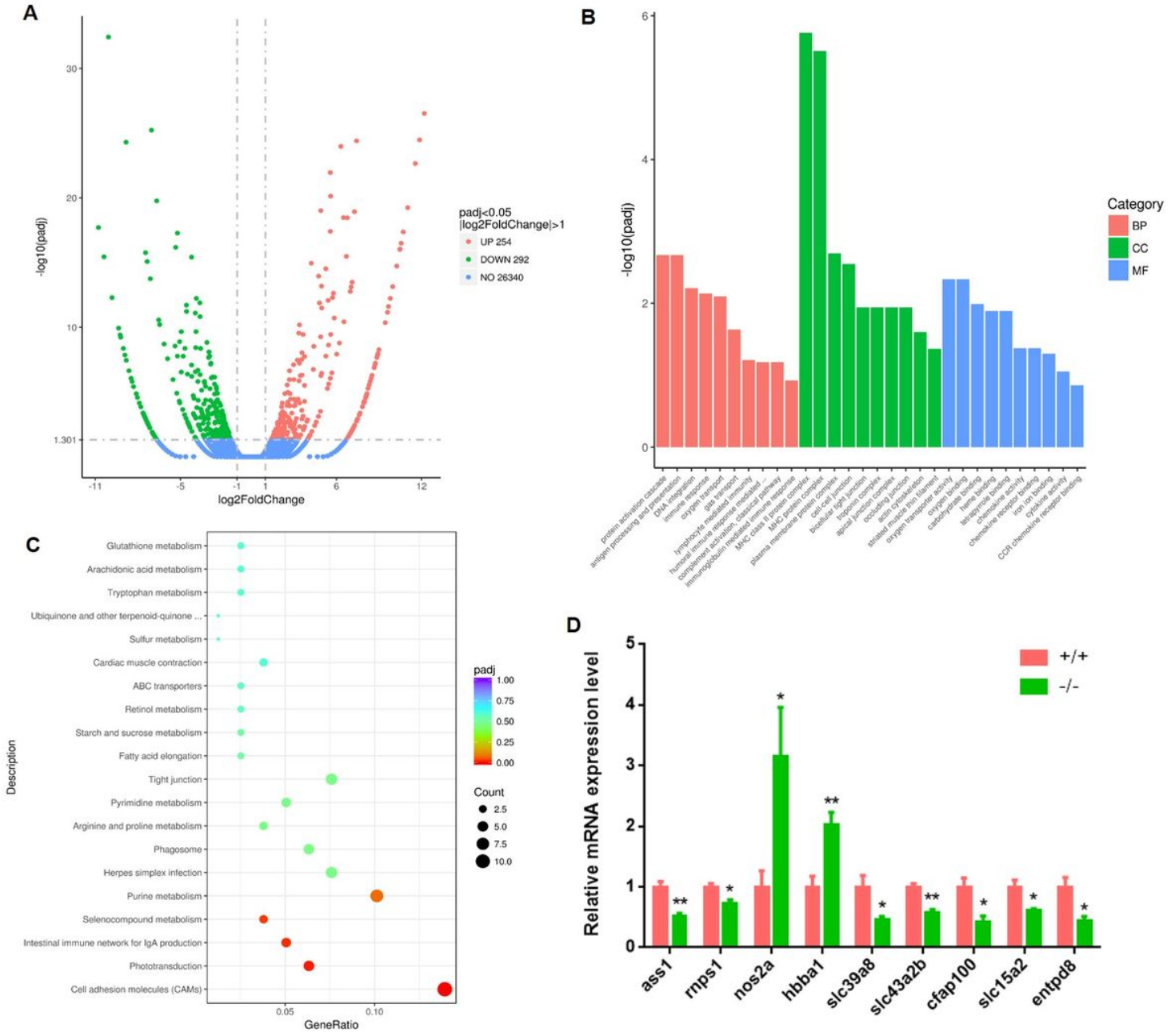

Figure 7

Transcriptome sequencing analysis of nomo1 mutant zebrafish. (A) Volcano map of DEGs between WT and nomo1-/- zebrafish. The abscissa and ordinate indicate the fold change in expression of DEGs (log2fold change) and the significance level of the DEGs (-log10padj) between WT and mutant zebrafish, respectively. The upregulated genes are indicated by a red dot, and the downregulated genes are indicated by a green dot. The significant level of enrichment (padj) was set as the multihypothesis test-corrected p-value (p-value< 0.05). (B) Chart showing differential expression and GO annotation classification. The horizontal coordinate is the GO term, and the vertical coordinate is the significance level of GO term enrichment. A higher value indicates a more significant enrichment. Different colors indicate the three GO subclasses: BP (biological process), CC (cellular component) and MF (molecular function). (C) KEGG pathway analysis of DEGs. Advanced bubble chart showing the enrichment of DEGs in signaling pathways. The vertical axis indicates the pathway, and horizontal axis indicates the gene ratio (gene ratio is the ratio of the number of DEGs to the total number of DEGs annotated to the KEGG pathway). The size and color of the bubble represent the number of DEGs enriched in a pathway and the significance of enrichment, respectively. (D) Representative experimental validation of DEGs by the RT-qPCR analysis. Gene expression is presented as the mean ± SEM, and a t-test was performed to compare gene expression between WT and nomo1-/- zebrafish (*p < 0.05 and **p < 0.01, N = 1×10 groups each for WT and mutant zebrafish).

Supplementary Files

This is a list of supplementary files associated with this preprint. Click to download.

- Table.S1Primersareusedinthisstudy.docx
- Figure.S2Theforebrainmarkersonmutantzebrafish.jpg
- Figure.S3Thekinpreferencebehavior.jpg
- Table.S2ThelistedDEGsandpvalues.xlsx
- Figure.S1Morphologicalanalysisofnomo1zebrafish.jpg
- Video.S1WTsocialpreferencebehavior.mp4
- Video.S3WTshoalingbehavior.mp4
- Video.S2nomo1socialpreferencebehavior.mp4
- Video.S5backandforthmotions.mp4
- Video.S4nomo1shoalingbehavior.mp4
- Video.S6stereotypicmovement.mp4
- Video.S7largecirculармovement.mp4
- Video.S8WTkinpreferencebehavior.mp4
- Video.S9nomo1kinpreferencebehavior.mp4